



# Polymer Cancerostatics Targeted with an Antibody Fragment Bound via a Coiled Coil Motif: In Vivo Therapeutic Efficacy against Murine BCL1 Leukemia

Michal Pechar,\* Robert Pola, Olga Janoušková, Irena Siegllová, Vlastimil Král, Milan Fábry, Barbora Tomalová, and Marek Kovář

Dedicated to Professor Karel Ulbrich on the occasion of his 70th birthday.

A BCL1 leukemia-cell-targeted polymer–drug conjugate with a narrow molecular weight distribution consisting of an *N*-(2-hydroxypropyl)methacrylamide copolymer carrier and the anticancer drug pirarubicin is prepared by controlled radical copolymerization followed by metal-free click chemistry. A targeting recombinant single chain antibody fragment (scFv) derived from a B1 monoclonal antibody is attached noncovalently to the polymer carrier via a coiled coil interaction between two complementary peptides. Two pairs of coiled coil forming peptides (abbreviated KEK/EKE and KSK/ESE) are used as linkers between the polymer–pirarubicin conjugate and the targeting protein. The targeted polymer conjugate with the coiled coil linker KSK/ESE exhibits 4× better cell binding activity and 2× higher cytotoxicity in vitro compared with the other conjugate. Treatment of mice with established BCL1 leukemia using the scFv-targeted polymer conjugate leads to a markedly prolonged survival time of the experimental animals compared with the treatment using the free drug and the nontargeted polymer–pirarubicin conjugate.

## 1. Introduction

The application of polymer–cancerostatic conjugates for neoplastic treatment provides several significant advantages compared with conventional chemotherapy. The polymer therapeutics usually exhibit much lower nonspecific toxicity against healthy cells and tissues as the biologically active molecules are preferentially released from the conjugates into the target tumor tissue or cells. The increased accumulation of the

polymer conjugates in solid tumors resulting from the enhanced permeation and retention (EPR) effect further improves the tumor selectivity of the polymer therapeutics.<sup>[1]</sup> Additionally, the polymer carrier enables the attachment of various targeting ligands that actively target cancer cells.<sup>[2–6]</sup>

Unfortunately, the EPR effect can be utilized only in the treatment of solid vascularized tumors. In other cases, such as the treatment of blood malignancies or metastases in early stages, the active targeting of the polymer therapeutics is highly desirable to improve the overall therapeutic efficiency. Among the various ligands that have been described to actively target cancer cells, antibodies and their fragments thus far appear to be the most efficient.<sup>[2,7–9]</sup>

However, the well-defined covalent conjugation of proteins to polymers is not easily accomplished. The reaction between proteins and reactive polymer precursors often results in a mixture of poorly defined products with a compromised biological activity. Therefore, there is an urgent need for conjugation methods that provide well-defined products with fully preserved biological activities.

Although several sophisticated methods to achieve the site-specific covalent modification of proteins have been recently described,<sup>[10–14]</sup> the formation of a specific noncovalent bond between two peptide tags is an equally attractive approach. Among the various noncovalent methods, the utilization of coiled coil heterodimers,<sup>[15–20]</sup> the hybridization of complementary morpholino oligonucleotides<sup>[21–23]</sup> and the formation of a complex between bungarotoxin and a bungarotoxin-binding peptide<sup>[24]</sup> for the attachment of biologically active proteins to polymer carriers are particularly notable.

The use of coiled coil heterodimers for preparation of polymer–drug conjugates containing either a biologically active protein (FosW<sub>C</sub> peptide)<sup>[16]</sup> or a low molecular weight cytostatic drug (methotrexate)<sup>[18]</sup> emerged in the literature after 2010.

Recently, we have reported the synthesis and in vitro evaluation of an *N*-(2-hydroxypropyl)methacrylamide (HPMA)-based polymer conjugate with an anticancer drug doxorubicin (Dox) targeted to murine leukemia BCL1 via a recombinant single

Dr. M. Pechar, Dr. R. Pola, Dr. O. Janoušková  
Institute of Macromolecular Chemistry  
Czech Academy of Sciences  
Heyrovského nám. 2, 162 06 Prague 6, Czech Republic  
E-mail: pechar@imc.cas.cz

I. Siegllová, Dr. V. Král, Dr. M. Fábry  
Institute of Molecular Genetics  
Czech Academy of Sciences  
Flemingovo nám. 2, 166 10 Prague 6, Czech Republic

B. Tomalová, Dr. M. Kovář  
Institute of Microbiology  
Czech Academy of Sciences  
Videňská 1083, 142 20 Prague 4, Czech Republic

DOI: 10.1002/mabi.201700173

chain fragment (scFv) of the monoclonal antibody B1.<sup>[25]</sup> The targeting protein was attached to the polymer–drug conjugate via a noncovalent interaction between two peptides that formed a coiled coil heterodimer. The scFv-targeted polymer conjugate exhibited almost 100 times higher cytotoxicity against BCL1 cells compared with the corresponding nontargeted polymer conjugate.

We have further optimized the structure of the targeted macromolecular therapeutic using a modified method to synthesize the polymer carrier, employing an improved structure of the coiled coil heterodimer between the polymer and the targeting protein<sup>[26]</sup> and introducing pirarubicin (Pir) instead of doxorubicin as a cytostatic drug.<sup>[27]</sup> In this paper, we describe the synthesis, results of physicochemical characterization and both in vitro and in vivo biological evaluations of the optimized HPMA-based polymer system using a BCL1 leukemia model.

## 2. Experimental Section

### 2.1. Materials and Methods

3-[2-[2-[2-(2-Azidoethoxy)ethoxy]ethoxy]ethoxy]propanoic acid (N<sub>3</sub>-PEG<sub>4</sub>-COOH) and N-[2-[2-[2-(2-azidoethoxy)ethoxy]ethyl]-biotinamide (N<sub>3</sub>-PEG<sub>3</sub>-biotin) were purchased from Click Chemistry Tools, USA. (RS)-1-Aminopropan-2-ol, 2,2'-azobis(2-methylpropionitrile) (AIBN), 4-cyano-4-thiobenzoylsulfanylpentanoic acid (CTP), 1-ethyl-3-(3-dimethylamino-propyl)carbodiimide (EDC), N,N-dimethylacetamide (DMA), 4-dimethylaminopyridine (DMAP), dimethyl sulfoxide (DMSO), methacryloyl chloride, *tert*-butanol, triisopropylsilane (TIPS), and trifluoroacetic acid (TFA) were purchased from Sigma-Aldrich (Sigma-Aldrich, Czech Republic). 3-Amino-1-(11,12-didehydrodibenzo[b,f]azocin-5(6H)-yl)propan-1-one (DBCO-NH<sub>2</sub>) was purchased from Click Chemistry Tools (AZ, USA). Pirarubicin (Pir) was obtained from Meiji Seika Pharma Co., Ltd. (Japan). All other chemicals and solvents were of analytical grade. Solvents were dried and purified by conventional procedures and distilled before use.

### 2.2. HPLC Monitoring of Polymer–Analogous Reactions

Monitoring of the conjugation reactions of DBCO-NH<sub>2</sub>, pirarubicin, biotin, and peptides to the reactive polymer precursors was performed by HPLC using a 100 × 4.6 mm Chromolith Performance RP-18e column (Merck, Germany) and a linear gradient of water–acetonitrile (0–100% acetonitrile) in the presence of 0.1% TFA with a UV–vis diode array detector (Shimadzu, Japan).

### 2.3. Cell Lines

BCL1 cell line was obtained from Prof. Blanka Říhová (Institute of Microbiology, Czech Academy of Sciences). The cells were cultivated in RPMI medium (Thermo Scientific, Czech Republic) supplemented with heat inactivated 10% fetal bovine serum (FCS), 100 U mL<sup>-1</sup> penicillin, 100 µg mL<sup>-1</sup> streptomycin, and 0.05 × 10<sup>-3</sup> M 2-sulfanylethanol.

**Table 1.** Basic characteristics of the copolymers.

Copolymer	$M_w^a)$	$M_w/M_n^a)$	TT [mol%] <sup>b)</sup>	Pir [wt%] <sup>c)</sup>	Peptide [wt%] <sup>d)</sup>	Biotin [wt%] <sup>d)</sup>
P <sub>TT</sub>	46 300	1.28	6.8	–	–	–
P <sub>Pir</sub>	59 700	1.19	–	9.6	–	–
P <sub>EKE</sub>	61 500	1.15	–	8.0	14.2	2.0
P <sub>ESE</sub>	62 000	1.13	–	8.1	13.8	2.1

<sup>a)</sup>Molecular weights determined by SEC using RI and LS detection; <sup>b)</sup>TT determined by UV–vis spectrophotometry in methanol ( $\epsilon_{305} = 10\,300\text{ L mol}^{-1}\text{ cm}^{-1}$ ); <sup>c)</sup>Pir determined by UV–vis spectrophotometry in methanol ( $\epsilon_{488} = 11\,300\text{ L mol}^{-1}\text{ cm}^{-1}$ ); <sup>d)</sup>Determined by HPLC analysis.

### 2.4. Size-Exclusion Chromatography (SEC)

The molecular weights and dispersity values of the polymers and polymer–Pir conjugates were determined by SEC on a Shimadzu HPLC system equipped with UV–vis diode array detector (Shimadzu, Japan), refractive index Optilab-rEX, and multi-angle light scattering DAWN EOS detectors (Wyatt Technology Corp., Santa Barbara, CA). TSK-Gel SuperAW3000 column and 80% methanol/20% sodium acetate buffer (0.3 M, pH 6.5) as an eluent at a flow rate of 0.6 mL min<sup>-1</sup> were used in all experiments. A method based on the known total injected mass with an assumption of 100% recovery was used to calculate of the molecular weights from the light scattering data. The number- and weight-average molecular weights for the polymer precursors and the polymer–Pir conjugates are summarized in Table 1.

### 2.5. UV–Vis Spectrophotometry

The spectrophotometric analyses were carried out in quartz glass cuvettes on a Helios Alpha UV–vis spectrophotometer (Thermospectronic, UK). The content of dithiobenzoate (DTB) end groups in the polymers were determined at 302 nm in methanol using the molar absorption coefficient  $\epsilon_{\text{DTB}} = 12\,100\text{ L mol}^{-1}\text{ cm}^{-1}$ . The results are summarized in Table 1. The determination of the Pir content in the polymer–Pir conjugates (without fluorophore) was performed at 488 nm in methanol using the molar absorption coefficient  $\epsilon_{\text{Pir}} = 11\,300\text{ L mol}^{-1}\text{ cm}^{-1}$ . The Pir contents are summarized in Table 2. The contents of carbonylthiazolidine-2-thione (TT) reactive groups in the polymer precursors were determined at 305 nm in methanol using the molar absorption

**Table 2.** Cytostatic activity of the scFv-targeted and nontargeted polymer–Pir conjugates and free Pir.

Sample	IC <sub>50</sub> (±SD) <sup>a)</sup>
P <sub>ESE</sub> /scFv <sub>KSK</sub>	9 ± 2
P <sub>EKE</sub> /scFv <sub>KEK</sub>	18 ± 3
P <sub>ESE</sub> /scFv <sub>0</sub>	89 ± 2
P <sub>EKE</sub> /scFv <sub>0</sub>	146 ± 2
Pir	1 ± 0.2

<sup>a)</sup>IC<sub>50</sub> (µg L<sup>-1</sup>), concentration of Pir equivalent in the sample inhibiting growth of the 50% cells compared with the untreated control.

coefficient  $\varepsilon_{\text{TT}} = 10\,300\text{ L mol}^{-1}\text{ cm}^{-1}$ . The contents of aza-dibenzocyclooctyne (DBCO) groups in the copolymers were determined at 292 nm using the absorption coefficient for DBCO in methanol,  $\varepsilon_{292} = 13\,000\text{ L mol}^{-1}\text{ cm}^{-1}$ .

## 2.6. Dynamic Light Scattering (DLS)

The hydrodynamic radii and scattering intensities of the polymer precursors and polymer conjugates were measured using the DLS technique at a scattering angle of  $\theta = 173^\circ$  on a Nano-ZS instrument (Model ZEN3600, Malvern Instruments, UK) equipped with a 632.8 nm laser. The measurements were performed in 0.012 M phosphate buffer with 0.138 M NaCl (PBS) (1.0 mg mL<sup>-1</sup>, pH 7.4) solutions. For the evaluation of the dynamic light scattering data, the DTS (Nano) program was used. The mean of at least three independent measurements was calculated.

## 2.7. Synthesis of Peptides EKE and ESE

The EKE and ESE peptides were prepared as described previously.<sup>[26]</sup>

## 2.8. Synthesis of Monomers

HPMA and Ma-GFLG-OH were prepared as described earlier.<sup>[28,25]</sup> Ma-GFLG-TT was prepared by reacting Ma-GFLG-OH (92 mg, 0.2 mmol) with 4,5-dihydrothiazole-2-thiol (29 mg, 0.24 mmol) using 1-ethyl-3-(3-dimethylaminopropyl)carbodiimide hydrochloride (57.5 mg, 0.3 mmol) in DMF in the presence of 4-dimethylaminopyridine at 4 °C overnight. After DMF was evaporated, the reaction mixture was dissolved in DCM and the water-soluble urea derivative was removed by subsequent washing of the organic solution with an aqueous solution of KHSO<sub>4</sub>, with a solution of NaCl and with water. After DCM was evaporated, the product was dried to yield 80 mg of the monomer, which was then characterized by HPLC (single peak) and MS ESI (calculated 561.7, found 562.9 M+H).

## 2.9. Synthesis of Polymer Precursor

Reversible addition-fragmentation chain transfer (RAFT) polymerization was performed as described earlier.<sup>[29]</sup> A monomer/CTA/initiator molar ratio of 1000:2:1 was used. HPMA (90 mol%, 100 mg), Ma-GFLG-TT (10 mol%, 43.6 mg) treated with the initiator ABIN (1.3 mg), and the chain transfer agent 4-cyano-4-thiobenzoylsulfanylpentanoic acid (1.06 mg) were mixed in DMA and tert-butyl alcohol (50/50 v/v). After removal of dithiobenzoate (DTB)  $\omega$ -end groups,<sup>[30]</sup> the polymer precursor P<sub>TT</sub> was characterized by SEC ( $M_w = 46\,300$ ,  $M_w/M_n = 1.28$ ) and the content of TT groups (6.8 mol%) was determined by UV-vis.

## 2.10. Synthesis of Polymer Conjugates

The polymer precursor P<sub>TT</sub> (90 mg, 0.033 mmol TT, i.e., 6.3 mol%) was dissolved in 1.5 mL of DMA and mixed with

pirarubicin (10 mg, 0.016 mmol) in 0.5 mL DMA. After 2 h, no remaining free drug was detected by HPLC. DBCO-NH<sub>2</sub> (5.8 mg, 0.021 mmol) was added and the reaction was left overnight. HPLC revealed a small amount of remaining DBCO-NH<sub>2</sub> and no TT groups on the polymer. The reaction mixture was precipitated into ethyl acetate; the crude polymer was dissolved in methanol and re-precipitated into ethyl acetate to yield the polymer-drug conjugate P<sub>Pir</sub>. The polymer was characterized using UV-vis to determine the amount of Pir (9.6 wt%).

The conjugation of the EKE or ESE peptide (1 mol%) to P<sub>Pir</sub> in DMA was monitored by HPLC, and the reaction was completed in 5 min. Then, N<sub>3</sub>-PEG<sub>3</sub>-biotin (1 mol%) was attached to the polymer and the remaining DBCO groups were end-capped with two molar excesses of N<sub>3</sub>-PEG<sub>4</sub>-COOH. The mixture was precipitated into acetone; the crude product was dissolved in methanol and re-precipitated into acetone to yield the polymer-drug-peptide conjugates P<sub>EKE</sub> and P<sub>ESE</sub>.

The contents of unbound Pir and peptides in the polymer conjugates (measured by HPLC analysis) were below 0.2% and 0.4% w/w of their total amount, respectively.

## 2.11. Preparation of Recombinant Proteins and ScFv-Targeted Polymer Conjugates

The scFv B1 fragment with a C-terminal KSK tag was obtained using a similar method as that used previously<sup>[17,25]</sup> for scFv B1 tagged with KEK. The difference between the KEK and KSK tags was that the design of KSK was improved; namely, IAALK-SKIAALKSE-(IAALKSK)<sub>2</sub> ensured the formation of an antiparallel coiled coil with a suitable polymer-bound counterpart.<sup>[26]</sup> Briefly, the 90 bp oligonucleotide duplex was prepared from four oligonucleotides:

SK1 = 5'-gtactatcgcagcgtgaaatctaagattgcccgtctgaaa,  
SK2 = 5'-tccgagatcgcggcactgaaatctaagatcggcctctgaaaagcaagg,  
SK3 = 5'-tgccgcatctcggatttcaaggccgcaatctagatttcagcgtcggata,  
and  
SK4 = 5'-gtaccctgcttttcagagcggcgtacttagatttcag,

where SK2 and SK3 partly overlapped and had their 5' ends phosphorylated, and where the 5' ends of SK1 and SK4 contained four-base overhangs to allow for cloning into the Acc65I site. The oligonucleotides SK1 + SK3 and SK2 + SK4 were annealed, the resulting duplexes were ligated, and the 90 bp KSK oligonucleotide duplex was gel-purified and used to replace the KEK tag in scFv B1. The final construct thus encoded scFv B1 in the format of VH-(gly4ser)4-VL-myc-KSK tag-His5.

## 2.12. Expression and Purification of the Fusion Protein scFv B1-KSK

For expression in *E. coli* BL21(DE3) cells, a modified pET-22(b) vector was used. In this vector, the scFv coding sequence is preceded by the PelB signal sequence, which allows for translocation of the product into the periplasmic space. The His5 tag at the C-terminus of the polypeptide was used for product isolation and purification by IMAC chromatography on

Ni-CAM (Sigma). The final purification was achieved by ion exchange chromatography on a MonoS column.<sup>[17,25]</sup>

### 2.13. In Vitro Cytotoxic Activity of the Polymer Conjugates

The cells ( $5 \times 10^3$ ) were seeded into 100  $\mu\text{L}$  of media in 96-well flat-bottom plates 24 h before the addition of free Pir or before the polymer conjugates  $\text{P}_{\text{ESE}}$  or  $\text{P}_{\text{EKE}}$  were dissolved in the solution of recombinant scFv fragments of the B1 antibody. These antibody fragments varied based on the presence of the coiled coil tags (KEK or KSK) or the absence of the tags ( $\text{scFv}_{\text{KEK}}$ ,  $\text{scFv}_{\text{KSK}}$ , and  $\text{scFv}_0$ , respectively, concentration 3.16  $\text{mg mL}^{-1}$ ). The polymer/protein weight ratio of 2:1, which corresponded to an ESE/KSK (or EKE/KEK) molar ratio of 3:1, was used. The concentrations of the  $\text{P}_{\text{ESE}}$  and  $\text{P}_{\text{EKE}}$  conjugates dissolved in the solutions of scFv fragments for the cytotoxicity testing varied from 0.02 to 100  $\mu\text{g mL}^{-1}$ . The drug concentrations of free Pir varied from 0.001 to 5  $\mu\text{g mL}^{-1}$  for the cytotoxicity testing. The cells were subsequently cultivated for 72 h in 5%  $\text{CO}_2$  at 37 °C. Then, 10  $\mu\text{L}$  of Alamar Blue cell viability reagent was added to each well, and the plates were incubated for 4 h at 37 °C. The metabolic activity was measured according to the protocol for the Synergy Neo plate reader (Bio-Tek, Czech Republic) using an excitation wavelength of 570 nm and an emission wavelength of 600 nm. As a control, the cells cultivated in medium without any treatment were employed. The assay was conducted in triplicate and repeated three times independently.

### 2.14. In Vitro Cell Binding Studies

To determine the binding of the  $\text{scFv}_{\text{KEK/KSK}}$ -targeted  $\text{P}_{\text{EKE/ESE}}$  conjugates to the cell membrane, the cells were washed with 0.5% bovine serum albumin in PBS (BSA–PBS) and  $\approx 2.5 \times 10^5$  of cells in a 50  $\mu\text{L}$  volume were incubated for 30 min at 25 °C with  $\text{P}_{\text{ESE/scFv}_{\text{KSK}}}$ ,  $\text{P}_{\text{EKE/scFv}_{\text{KEK}}}$  or  $\text{P}_{\text{ESE/scFv}_0}$ ,  $\text{P}_{\text{EKE/scFv}_0}$  (as a control). The conjugates with scFv were prepared as described above using a polymer/protein weight ratio of 2:1. The final concentration of scFv for the binding studies was 50  $\mu\text{g mL}^{-1}$ . Then, the cells were washed with 0.5% BSA–PBS, diluted in 50  $\mu\text{L}$ , and labeled for 30 min in the dark at 25 °C with streptavidin-Alexa 405 (Thermo Scientific, Czech Republic), which recognizes biotin on conjugates, and anti-c-Myc-fluorescein (Exbio, Czech Republic), which recognizes the Myc tag sequence in scFv. Afterward, the cells were washed with 0.5% BSA–PBS and diluted in 0.5 mL of 0.5% BSA–PBS containing 1  $\mu\text{g mL}^{-1}$  7-AAD to detect dead cells. The median fluorescence intensity of the polymer conjugates labeled with streptavidin-Alexa fluor 405 and scFv labeled with anti-c-Myc-fluorescein was determined. The samples were analyzed by FACS Verse (Becton Dickinson) and FlowJo software (TreeStar). The FACS analysis of the cell binding of the polymer conjugates was performed five times in triplicates.

### 2.15. Mice

Inbred BALB/c (*H-2<sup>d</sup>*) mice (females) were obtained from the animal breeding facility of the Institute of Physiology, Czech

Academy of Sciences. Mice were used at 9–15 weeks of age, and food and water were given ad libitum. In all animal works, institutional guidelines for the care and use of laboratory animals were strictly followed under a protocol approved by the Institutional Animal Care and Use Committee of the Czech Academy of Sciences and compliant with local and European guidelines.

### 2.16. Monoclonal Antibodies

The following monoclonal antibodies were used to stain surface antigens: anti-Myc-fluorescein (ExBio), CD3-biotin, CD3-eF450, CD4-PE, CD4-APC, CD4-FITC, CD80-APC, MHC II-PE, and STP-eF450 (eBiosciences). Live and dead cells were distinguished by propidium iodide staining.

### 2.17. Blood Clearance of the Polymer Conjugates

BALB/c mice were i.v. injected with the polymer–pirarubicin conjugate  $\text{P}_{\text{ESE/scFv}_{\text{KSK}}}$ , the polymer–pirarubicin conjugate  $\text{P}_{\text{ESE/scFv}_0}$ , or the same volume of PBS (220  $\mu\text{L}$ ). The dose of the conjugate corresponded to a dose of 75  $\mu\text{g}$  Pir per mouse. Samples of blood were taken from experimental mice at 1 min, 1, 6, 12, 24, and 48 h postinjection. Samples taken at 1 min, 12, and 48 h were taken from the carotid arteries and samples taken at 1, 6, and 24 h were taken from the tail vein. Blood samples were collected in heparinized microtubes and the plasma was separated. The concentration of Pir in the plasma samples was determined using HPLC analysis. The amount of Pir released from the polymer conjugate was determined after its extraction from the plasma into chloroform. Mixtures of 50  $\mu\text{L}$  of blood plasma samples and 50  $\mu\text{L}$  of 6 M HCl were heated to 50 °C for 1 h followed by extraction with 0.4 mL of chloroform for 15 min. The chloroform extract was evaporated to dryness and the residue was diluted with 0.5 mL of methanol. The Pir content was determined using an HPLC Shimadzu system equipped with a fluorescence detector with an excitation wavelength of 488 nm and an emission wavelength of 560 nm. The calibration was carried out using Pir standards dissolved in DMSO that were diluted with blood plasma, hydrolyzed with 6 M HCl and extracted with chloroform as described above.

### 2.18. In Vivo Binding Studies

BALB/c mice were i.p. inoculated with  $5 \times 10^5$  BCL1 cells in 250  $\mu\text{L}$  of PBS on day 0. The targeted polymer–pirarubicin conjugate  $\text{P}_{\text{ESE/scFv}_{\text{KSK}}}$  and the nontargeted control polymer conjugate  $\text{P}_{\text{ESE}}$  dissolved in PBS at concentrations of 6.2  $\text{mg mL}^{-1}$  (polymer conjugate) and 3.1  $\text{mg mL}^{-1}$  (scFv). These treatments were i.v. administered on day 30, and one dose contained 5  $\text{mg kg}^{-1}$  of polymer-bound Pir. The spleens were harvested 1, 2.5, 6, and 24 h after the administration of conjugates. Naïve mice, mice inoculated with BCL1 cells, and mice i.v. injected with PBS alone were used as controls. Each experimental group contained two mice.

## 2.19. Staining for Surface Antigens and Flow Cytometry

The spleens were harvested and homogenized using a gentleMACS Dissociator (Miltenyi Biotech) in flow cytometry buffer (PBS, 2% FCS,  $2 \times 10^{-3}$  M EDTA). The cell suspensions were filtered using a 70  $\mu$ m cell strainer (BD Biosciences), resuspended in flow cytometry buffer after red blood cell lysis with ACK lysing buffer (GIBCO), and filtered again using a 30  $\mu$ m cell strainer (BD Biosciences). The resultant cell suspensions were blocked by 20% mouse serum for 30 min on ice and stained with anti-c-Myc-fluorescein (Exbio, Czech Republic) for 30 min on ice in the dark. The cells were then washed twice in flow cytometry buffer, stained with streptavidin-eF450 (eBioscience, Czech Republic) for 20 min on ice in the dark and washed twice in flow cytometry buffer. Finally, the cells were stained with propidium iodide shortly before analysis on an LSR II flow cytometer (BD Biosciences). The data were analyzed using FlowJo software (Tree Star).

## 2.20. Treatment of Established BCL1 Leukemia In Vivo

BALB/c mice were i.p. inoculated with  $5 \times 10^5$  BCL1 cells in 250  $\mu$ L of PBS on day 0. The targeted polymer–Pir conjugate  $P_{ESE}/scFv_{KSK}$  and the nontargeted control polymer conjugate  $P_{ESE}$  were dissolved in PBS at concentrations of 6 mg mL<sup>-1</sup> (polymer conjugate) and 3 mg mL<sup>-1</sup> (scFv). The treatments were then i.v. administered in three doses on days 11, 14, and 17. One dose contained 5 mg kg<sup>-1</sup> of polymer-bound Pir. Another group of BALB/c mice were inoculated with BCL1 cells and treated with free Pir on days 11, 14, and 17. One dose contained 3.5 mg kg<sup>-1</sup> Pir (estimated as equitoxic to 5 mg kg<sup>-1</sup> of polymer-bound Pir) in PBS with 2% of DMSO at a concentration of 0.34 mg mL<sup>-1</sup>. BALB/c mice inoculated with BCL1 cells and injected with PBS on days 11, 14, and 17 were used as the control group. Tumor progression and general fitness of the mice were checked every second day, and the body weight and survival of the mice were recorded. Each experimental group included eight mice.

## 2.21. Statistical Analysis

Statistical analysis was performed using the Log-rank test (survival graphs) or ANOVA, followed by Tukey's multiple comparison test; \*, \*\* and \*\*\* represent *p*-values <0.05, 0.01, and 0.001, respectively. The data were representative of at least two experiments.

# 3. Results and Discussion

## 3.1. Synthesis of the Peptides and Polymer Conjugates

In our previous work,<sup>[26]</sup> we compared the associative behavior of two pairs of coiled coil peptides: (VAALEKE)<sub>4</sub>/(VAALKEK)<sub>4</sub> (EKE/KEK) formed coiled coil heterodimers with randomly oriented peptide chains, whereas (IAALESE)<sub>2</sub>-IAALESKIAALESE/IAALKSKIAALKSE-(IAALKSK)<sub>2</sub> (ESE/KSK) formed higher

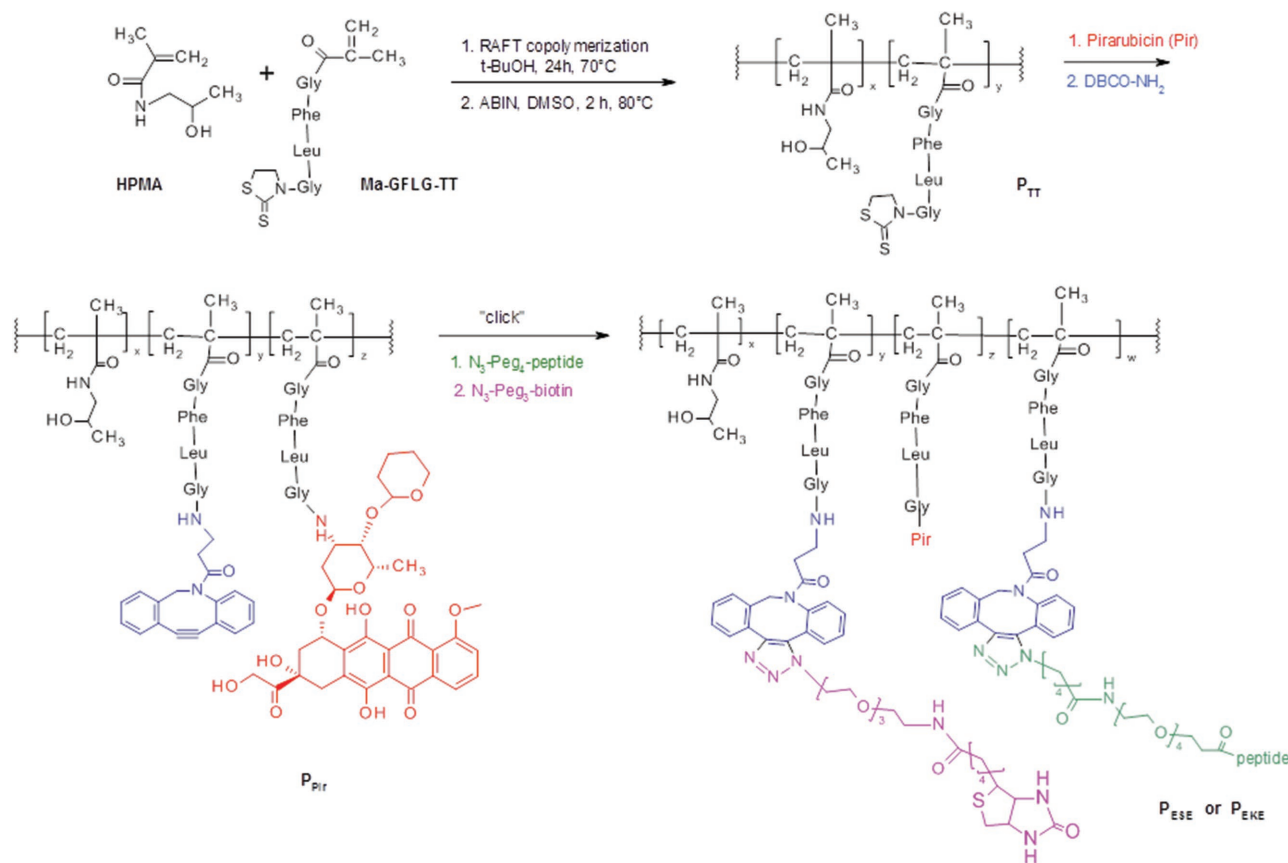
heterooligomers with antiparallel orientations of the peptides and stronger binding activities. Though it is not possible to describe the formation of the coiled coil oligomers using a single binding constant due to the multi-step characteristics of the process, the higher stability of the latter pair was evident from the following observations. While the individual peptides EKE and KEK had random coil conformations and adopted the coiled coil conformation only upon mixing of the two peptides ( $\alpha$ -helix melting  $T_m > 61$  °C), the peptides ESE and KSK already exhibited high helical contents as individual peptides, and upon mixing of the two components, the stability of the coiled coil was further increased ( $T_m > 95$  °C). We hypothesized that the latter pair of peptides would be more suitable for attachment of a targeting ligand to the polymer drug carrier due to the higher stability of the coiled coil and due to the antiparallel orientation of the peptide chains that would minimize eventual steric hindrance.

Compared with our previous work, we have improved the synthesis of the polymer precursors in order to obtain polymer carriers with low dispersity (<1.2). Specifically, we used RAFT copolymerization of HPMa with 3-(*N*-methacryloylglycylphenylalanylleucylglycyl)thiazolidine-2-thione (Ma-GFLG-TT). The resulting reactive copolymer  $P_{TT}$  was submitted to reaction with a cytostatic drug pirarubicin (Pir), and the remaining TT groups were aminolyzed with an amino derivative of dibenzocyclooctyne (DBCO-NH<sub>2</sub>) to yield the polymer precursor  $P_{Pir}$  (Scheme 1).

The coiled coil-forming peptides with *N*-terminal azide groups were designed and synthesized as described in our previous publications.<sup>[17,25,26]</sup> The peptide azides (EKE and ESE) were bound to the polymer precursor  $P_{Pir}$  via metal-free azide-alkyne cycloaddition (“click” chemistry) utilizing the reaction between DBCO groups of the polymer precursor and the azide functions of the peptides. Another part of DBCO groups was modified with an azide derivative of biotin to enable monitoring of the fate of the polymer carrier both in vitro and in vivo. The remaining DBCO groups were end-capped with N<sub>3</sub>-PEG<sub>4</sub>-COOH to yield the polymer–drug–peptide conjugates  $P_{EKE}$  and  $P_{ESE}$ , which contained the peptides EKE and ESE, respectively (Scheme 1).

The basic physicochemical characteristics of all of the prepared copolymers are summarized in Table 1. SEC chromatogram of the polymer–pirarubicin conjugate  $P_{ESE}$  is shown in Figure S2 (Supporting Information) as an example.

The low dispersity value of the copolymers is an important feature of the presented polymer drug delivery system. It has been repeatedly reported that the pharmacokinetic behavior of a polymer therapeutic is significantly influenced by both its molecular weight and dispersity. Polymers with a broad distribution of molecular weights contain a fraction of smaller macromolecules with shorter blood circulation times and lower levels of accumulation in solid tumors, whereas a fraction of larger macromolecules show longer blood circulation times and higher levels of tumor accumulation due to the EPR effect. If the molecular weight of the largest macromolecules exceeds the renal threshold, they cannot be eliminated via glomerular filtration and may remain in organism for extended periods of time, with unknown physiological effects.<sup>[31]</sup> Consequently, only a limited fraction of such polydispersed polymeric drugs



**Scheme 1.** Synthesis of the polymer–drug–peptide conjugates P<sub>EKE</sub> and P<sub>ESE</sub>.

have the optimal pharmacokinetic and therapeutic profiles. In contrast, we can speculate that macromolecular therapeutics with low dispersity (e.g., originating from RAFT polymerization) should exhibit more uniform pharmacokinetics and, consequently, better therapeutic efficacy. Nevertheless, it should be noted that this is just a hypothesis, and there is not yet enough experimental in vivo data available in the literature to support this statement.

### 3.2. Preparation of Recombinant Proteins and scFv-Targeted Polymer Conjugates

The recombinant scFv fragments of the B1 antibody with either the KEK or KSK coiled coil tag or without the tag (scFv<sub>KEK</sub>, scFv<sub>ESE</sub>, and scFv<sub>0</sub>, respectively) were expressed and isolated from *E. coli*, as described earlier. The purified proteins in PBS buffer (pH 7.4) were mixed with the corresponding complementary polymer conjugates to yield the scFv-targeted supramolecular complexes P<sub>EKE</sub>/scFv<sub>KEK</sub> and P<sub>ESE</sub>/scFv<sub>KSK</sub>. The molar ratio of EKE/KEK (and ESE/KSK) was set to 3:1, which corresponds to a polymer/protein weight ratio of 2:1. In addition to the physicochemical methods (size-exclusion chromatography and sedimentation analysis) described in our previous papers, the formation of the supramolecular complexes polymer–protein was also confirmed by dynamic light scattering (Figure 1).

### 3.3. In Vitro Binding Studies

The in vitro binding efficacy of the targeted polymer conjugates P<sub>EKE</sub>/scFv<sub>KEK</sub> and P<sub>ESE</sub>/scFv<sub>KSK</sub> or the polymer conjugate P<sub>EKE</sub> or P<sub>ESE</sub> mixed together with the targeting protein without the coiled coil-forming tag (P<sub>EKE</sub>/scFv<sub>0</sub>; P<sub>ESE</sub>/scFv<sub>0</sub>) was evaluated in BCL1 cells using flow cytometry. Figure 2A,B shows a representative example of the detection of scFv and the polymer backbone in the samples incubated with the targeted conjugates. We were able to detect similar anti-Myc-FITC signals originating from the targeting scFv in both targeted polymer conjugates (P<sub>EKE</sub>/scFv<sub>KEK</sub> and P<sub>ESE</sub>/scFv<sub>KSK</sub>). The binding of streptavidin-Alexa fluor 405 to the biotin-labeled targeted P<sub>ESE</sub>/scFv<sub>KSK</sub> conjugate showed a significantly higher median fluorescence intensity (MFI) of Alexa 405 (MFI 16 306) than P<sub>EKE</sub>/scFv<sub>KEK</sub> (MFI 3967). Figure 2C shows quantitative difference in MFI of Alexa 405 after binding streptavidin-Alexa fluor 405 to the biotin-labeled targeted P<sub>EKE</sub>/scFv<sub>KEK</sub> and P<sub>ESE</sub>/scFv<sub>KSK</sub> conjugates. In accordance with our original hypothesis and previously published<sup>[26]</sup> results, we attributed this difference in cell binding efficiency to the formation of antiparallel coiled coil heterodimers and to the stronger interactions between ESE/KSK peptides compared with the weaker, randomly oriented EKE/KEK coiled coils.

The cells incubated with the nontargeted polymers mixed with the control protein without the coiled coil tag (P<sub>EKE</sub>+scFv<sub>0</sub>; P<sub>ESE</sub>+scFv<sub>0</sub>) exhibited only the signal of scFv binding to the

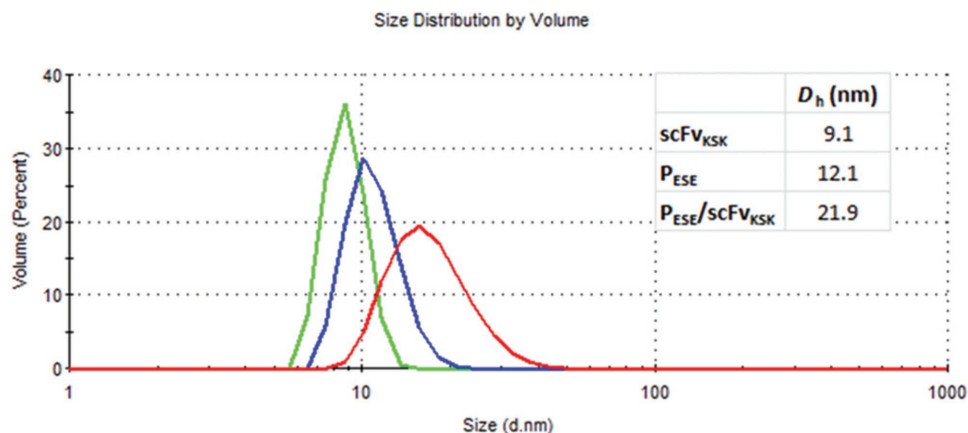


**Figure 1.** Particle size distribution and hydrodynamic diameters obtained by DLS analysis. Green line, scFv<sub>KSK</sub>; blue line, P<sub>ESE</sub>; red line, P<sub>ESE</sub>/scFv<sub>KSK</sub> complex.

cells, and no signal corresponding to the polymer was detected (data not shown).

### 3.4. Cytostatic Activity of the Polymer Conjugates In Vitro

In accordance with the results of flow cytometry cell binding studies, the in vitro evaluation of the cytotoxicity of the targeted conjugates revealed that the cytotoxicity of P<sub>ESE</sub>/scFv<sub>KSK</sub> was two times greater than that of P<sub>EKE</sub>/scFv<sub>KEK</sub> (Table 2). The targeted polymer conjugates P<sub>ESE</sub>/scFv<sub>KSK</sub> and P<sub>EKE</sub>/scFv<sub>KEK</sub>

exhibited cytotoxicities that were ten times and eight times higher, respectively, than those of the nontargeted conjugates P<sub>ESE</sub>/scFv<sub>0</sub> and P<sub>EKE</sub>/scFv<sub>0</sub>.

In general, the targeted polymer conjugates show significantly higher cytotoxic effects in vitro than the corresponding nontargeted conjugates. The cytotoxicities of both the nontargeted polymer conjugates differed only slightly, as P<sub>ESE</sub>/scFv<sub>0</sub> exhibited somewhat higher cytotoxic effects than P<sub>EKE</sub>/scFv<sub>0</sub>. We speculated that this difference might be explained by different interactions between the polymer-borne peptide sequences and the cell membrane. The dependence of the

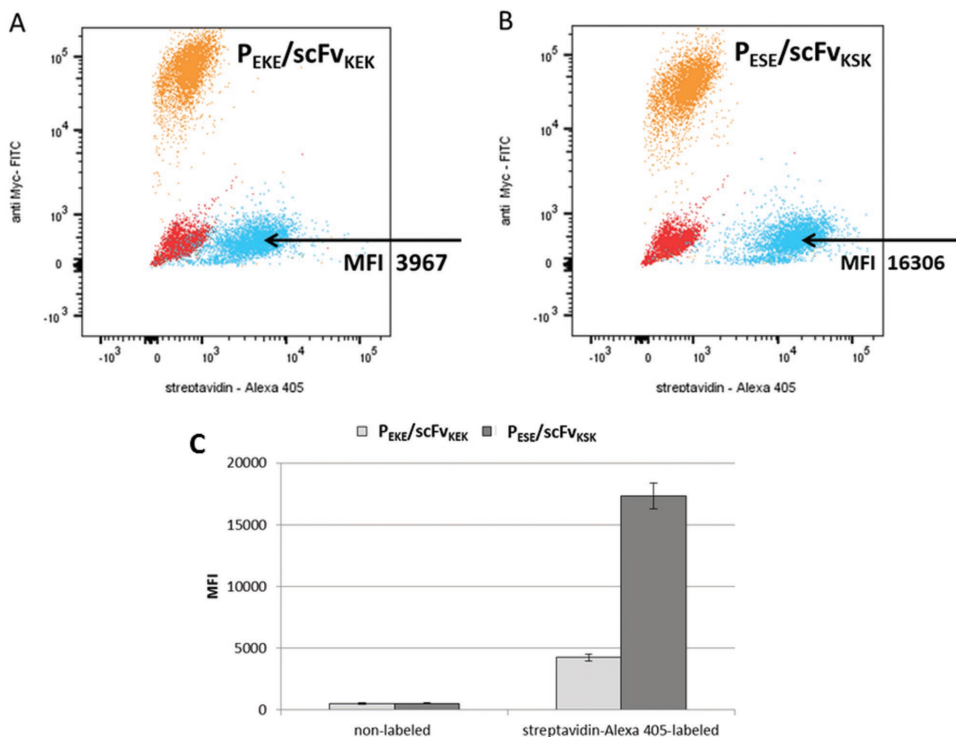


**Figure 2.** Flow cytometry analysis of BCL1 cell binding by the targeted conjugates A) P<sub>EKE</sub>/scFv<sub>KEK</sub> and B) P<sub>ESE</sub>/scFv<sub>KSK</sub>. Along the y-axis, the dot plot shows anti-Myc-FITC signals (orange) indicating the binding of scFv to the cells; along the x-axis, the streptavidin-Alexa 405 signal (blue) indicates the binding of the polymer to the cells and nonlabeled population of cells (red). C) Quantification of MFI of the cell binding experiment.

cell viability on the concentration of the polymer conjugates is shown in Figure S1 (Supporting Information). Free pirarubicin shows the highest cytotoxicity, which is a well-known fact from *in vitro* studies.<sup>[25,32,33]</sup> The advantages of polymeric drugs become evident *in vivo* due to their longer circulation times, decreased side effects and the possible presence of targeting ligands.

Based on the results of both the cell binding and cytotoxicity studies, the following *in vivo* experiments were performed using only the most efficient targeted polymer conjugate,  $P_{ESE}/scFv_{KSK}$ .

### 3.5. Blood Clearance of the Polymer Conjugates

The persistence of the conjugates in circulation was determined in BALB/c mice *i.v.* injected with the polymer–pirarubicin conjugate  $P_{ESE}/scFv_{KSK}$  or the polymer–pirarubicin conjugate  $P_{ESE} + scFv_0$ . The data showed that the majority ( $\approx 90\%$ ) of injected Pir disappeared from circulation within 6 h after the administration of polymeric conjugates (Figure 3). However, a small fraction of injected Pir (about 1%) was still detectable in the blood even 48 h after administration. At the 6 h time point, a slightly slower elimination rate of Pir from the circulation was seen when the polymeric conjugate associated with the targeting scFv was used in comparison to the use of the conjugate without scFv; however, this effect was diminished at later time points. The slower elimination of the scFv-targeted polymer conjugate can be most likely attributed to its higher molecular weight (and hydrodynamic volume) compared with that of the nontargeted polymer. The corresponding half-times  $T_{1/2\alpha}$  and  $T_{1/2\beta}$  characterizing the absorption and elimination phases of the pharmacokinetics of the both polymer conjugates together

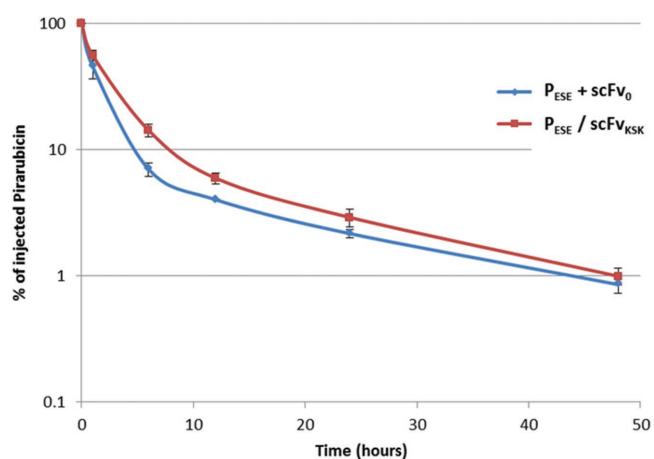


**Figure 3.** Pharmacokinetics of Pir in the blood of mice injected with targeted and nontargeted polymer–pirarubicin conjugates. BALB/c mice were *i.v.* injected with the targeted polymer–pirarubicin conjugate  $P_{ESE}/scFv_{KSK}$  (red line) or the nontargeted polymer conjugate  $P_{ESE}$  (blue line) mixed with  $scFv_0$  at doses equivalent to 75  $\mu\text{g}$  of pirarubicin. Blood was collected 1 min, 1, 6, 12, 24, and 48 h postinjection and was analyzed using HPLC. The concentration of Pir in the blood determined at 1 min after administration was considered 100%. Each experimental group included three mice.

with the biexponential functions used for the calculations are shown in Figure S3 (Supporting Information).

### 3.6. In Vivo Binding Studies

The ability of the targeted polymeric conjugate to bind to tumor cells *in vivo* was determined in BALB/c mice with developed BCL1 leukemia. Mice were *i.v.* injected with the targeted polymer–Pir conjugate  $P_{ESE}/scFv_{KSK}$  or the nontargeted polymer conjugate  $P_{ESE}$  mixed with scFv 30 d after inoculation with BCL1 cells, which ensured that the spleens of the experimental mice contained significant BCL1 tumor cell counts. BCL1 cells were identified by double positivity for MHC II and CD80, as BCL1 cells are known to strongly express these markers *in vivo*.<sup>[34]</sup> At selected time points after conjugate administration, the polymeric conjugates and scFv bound to the surface of BCL1 cells were detected in spleen cell suspensions using streptavidin-eF450 (as the polymer conjugates contained biotin) and anti-c-Myc mAb-FITC (as scFv contained the Myc tag), respectively. The BCL1 cells in mice injected with the polymer conjugate  $P_{ESE}$  mixed with  $scFv_0$  showed gradually increasing  $scFv_0$  binding for up to 6 h and much lower binding at 24 h (Figure 4). In contrast, the BCL1 cells in mice injected with the targeted polymer–Pir conjugate  $P_{ESE}/scFv_{KSK}$  showed very strong binding of both scFv and the polymer at 1 h postinjection. The binding was somewhat lower at 2.5 and 6 h postinjection and very low at 24 h postinjection (Figure 4). The sharp decrease in binding of the polymer conjugate targeted with scFv in comparison with free scFv after 24 h likely reflected the much stronger internalization of the multivalent polymer–Pir conjugate  $P_{ESE}/scFv_{KSK}$  complexes compared with that of monovalent scFv. Overall, we clearly demonstrated that  $scFv_{KSK}$  tightly binds to the polymer–Pir conjugate  $P_{ESE}$  and that the resulting targeted polymer–Pir conjugate  $P_{ESE}/scFv_{KSK}$  binds to the targeted BCL1 cells *in vivo* upon *i.v.* administration. Our targeted polymeric carrier bearing the cytostatic drug Pir is thus able to selectively deliver Pir to tumor cells in mice.

### 3.7. Treatment of Established BCL1 Leukemia In Vivo

The antitumor activities of the targeted polymer–pirarubicin conjugate  $P_{ESE}/scFv_{KSK}$  and the nontargeted control polymer conjugate  $P_{ESE}$  mixed with scFv was tested in a BCL1 leukemia mouse model with diffuse malignancy that did not form solid tumors. The mice were injected with tumor cells and the conjugates or free pirarubicin were administered in three separate doses on days 11, 14, and 17. Only the targeted polymeric conjugate therapy impeded the increase in body weight of the experimental mice, which is a sign of disease progression (Figure 5A). This result showed that only the targeted polymeric conjugate was capable of inhibiting the massive outbreak of the disease within the recorded time period (up to day 40). The median survival times were 36.5, 42.5, 45.5, and 66.5 d for the untreated mice, the mice treated with free pirarubicin, the mice injected with the nontargeted polymer and the mice injected with the targeted conjugate, respectively.

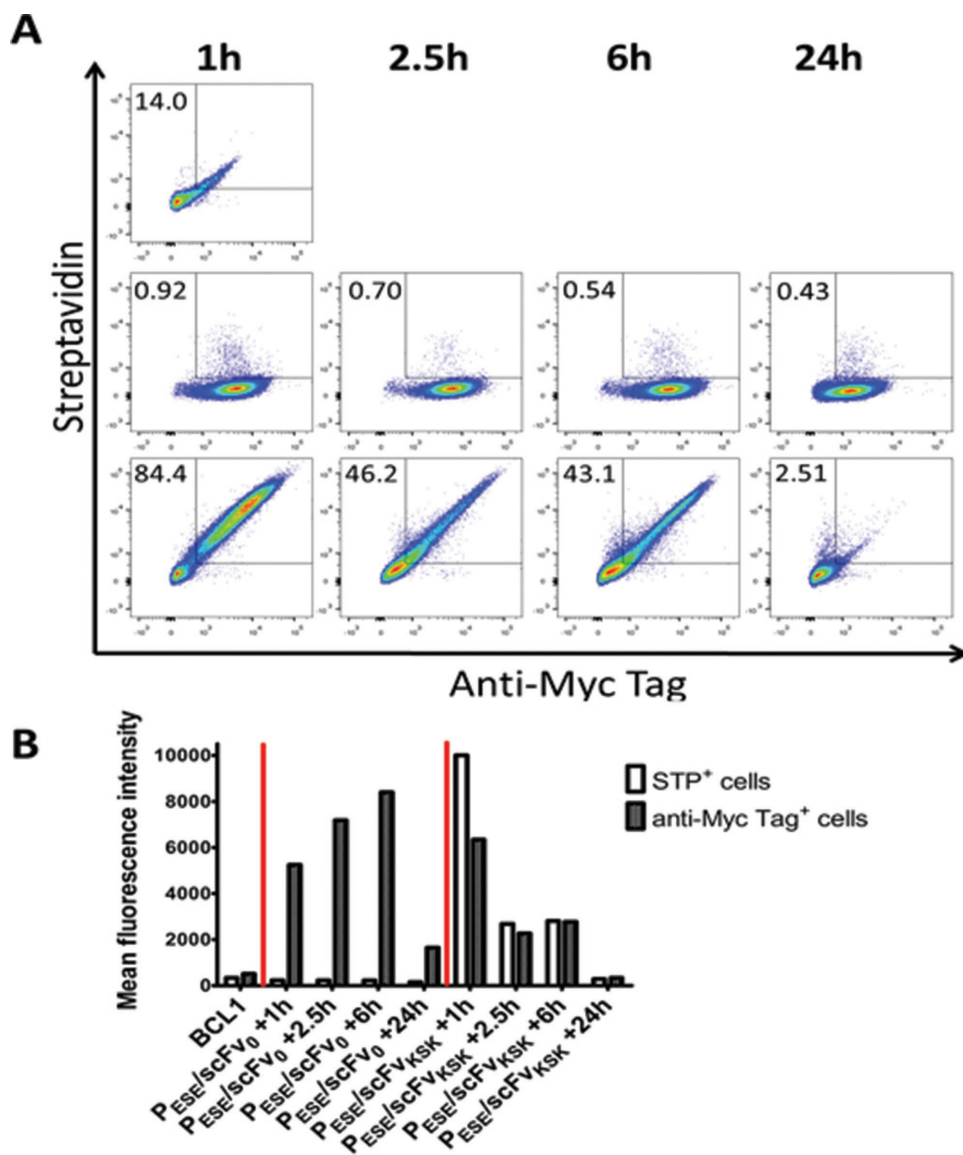


**Figure 4.** In vivo binding of targeted and nontargeted polymer-pirarubicin conjugates. BALB/c mice were i.p. injected with  $5 \times 10^5$  BCL1 cells on day 0. Mice were i.v. injected with the targeted polymer-pirarubicin conjugate P<sub>ESE</sub>/scFv<sub>KSK</sub> (P<sub>ESE</sub>/scFv<sub>KSK</sub>; 5 mg kg<sup>-1</sup> of polymer-bound pirarubicin per dose) or the nontargeted control polymer conjugate P<sub>ESE</sub> (P<sub>ESE</sub>; 5 mg kg<sup>-1</sup> of polymer-bound pirarubicin per dose) mixed with scFv on day 30. BALB/c mice bearing BCL1 leukemia (BCL1) and i.v. injected with PBS were used as controls. Spleens were harvested 1, 2.5, 6, and 24 h after the injection of polymeric conjugates. BCL1 cells were gated as MHC II<sup>+</sup> CD80<sup>+</sup> double positive cells. A) Dot plots showing binding of scFv (anti-Myc labeling) and polymeric conjugate (streptavidin labeling) to BCL1 cells. Each dot plot shows one representative mouse. The upper row shows a control mouse, the middle row shows mice injected with the polymer conjugate P<sub>ESE</sub> mixed with scFv<sub>0</sub>, and the lower row shows mice injected with the targeted polymer conjugate P<sub>ESE</sub>/scFv<sub>KSK</sub>. B) Mean fluorescence intensities of scFv binding (dark columns) and polymer conjugate binding (empty columns); each column shows one representative mouse from the group.

Both conjugates significantly prolonged the survival times of the experimental mice (Figure 5B) compared with both mice treated with the free drug and the untreated control. Though there was a statistically nonsignificant difference in the survival times of mice treated with the nontargeted and targeted conjugates, therapy with the targeted conjugate led to a complete cure in one experimental mouse and markedly prolonged survival of another five animals. Thus, the targeted polymeric conjugate proved to be the most efficient treatment modality, and the results reflected the ability of the targeted polymeric

conjugate to selectively deliver the cytostatic drug to the cancer cells.

#### 4. Conclusions

We synthesized hydrophilic polymer conjugates with narrow molecular weight distributions containing the anticancer drug pirarubicin bound to the polymer backbone via an enzymatically cleavable tetrapeptide spacer. A recombinant antibody fragment

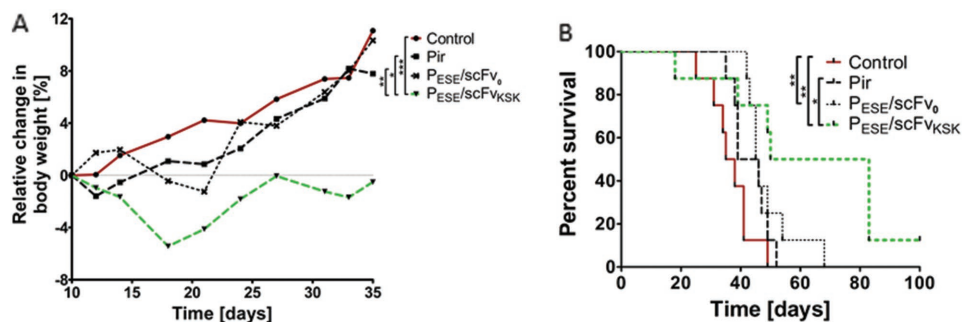


**Figure 5.** Treatment of BCL1 leukemia with polymer conjugates. BALB/c mice were i.p. injected with  $5 \times 10^5$  BCL1 cells on day 0. Mice were i.v. injected with three doses of targeted polymer–pirarubicin conjugate  $P_{ESE}/scFv_{KSK}$  ( $P_{ESE}/scFv_{KSK}$ ;  $5 \text{ mg kg}^{-1}$  of polymer-bound pirarubicin per dose), nontargeted control polymer conjugate  $P_{ESE}$  ( $P_{ESE}$ ;  $5 \text{ mg kg}^{-1}$  of polymer-bound pirarubicin per dose) mixed with  $scFv_0$ , or free pirarubicin (Pir;  $3.5 \text{ mg kg}^{-1}$ ) on days 11, 14, and 17. BALB/c mice injected with BCL1 cells and treated with PBS were used as controls. A) Changes in relative body weights of experimental mice. B) Survival of experimental mice. Groups were compared using ANOVA followed by A) Tukey's multiple comparison test or B) Log-rank test; \*, \*\*, and \*\*\* represent  $p$ -values  $< 0.05$ ,  $0.01$ , and  $0.001$ , respectively. Eight mice per group were used. The experiment was repeated twice with similar results.

that specifically binds to leukemia cells was attached to the polymer–drug conjugate via a universal noncovalent coiled coil interaction. The major advantage of the coiled coil approach compared with traditional covalent conjugation methods lies in the well-defined and absolutely nondestructive preparation of the polymer–protein complex. It was demonstrated that the choice of the coiled coil linker between the protein and the polymer can significantly affect both the cell binding efficiency of the targeted polymer–drug conjugate and its cytotoxic activity against the target malignant cells. The superior therapeutic efficiency of the scFv-targeted polymer cancerostatic compared with the low-molecular weight drug and the nontargeted polymer–drug conjugate was demonstrated in vivo using a murine BCL1 leukemia model.

We believe that targeted polymer cancerostatics utilizing noncovalent interactions of the two complementary peptides between the polymer carrier and the targeting protein ligand represent a highly promising new type of nanomedicine. The approach used herein might help to overcome not only the drawbacks of current chemotherapies, such as the general non-specific toxicity, but also frequent problems with the clinical approval of nanomedicines by regulatory authorities due to the low uniformity and poorly defined structures of polymer–protein conjugates prepared by more traditional covalent methods.

## Supporting Information

Supporting Information is available from the Wiley Online Library or from the author.

## Acknowledgements

This work was supported by the Ministry of Education, Youth and Sports of the Czech Republic within the National Sustainability Program I (project POLYMAT LO1507) and II (project BIOCEV-FAR LQ1604), by the Ministry of Health of the Czech Republic (project 16-28594A), and by the Czech Science Foundation (projects 16-17207S and 13-12885S).

## Conflict of Interest

The authors declare no conflict of interest.

## Keywords

cancer therapy, coiled coil, drug targeting, hydrophilic polymer, scFv

Received: May 16, 2017

Revised: July 17, 2017

Published online:

- [1] H. Maeda, H. Nakamura, J. Fang, *Adv. Drug Delivery Rev.* **2013**, *65*, 71.
- [2] J. Kopeček, Z.-R. Lu, P. Kopečková, *Nat. Biotechnol.* **1999**, *17*, 1101.
- [3] C. M. Ward, M. Pechar, D. Oupický, K. Ulbrich, L. W. Seymour, *J. Gene Med.* **2002**, *4*, 536.
- [4] R. Pola, M. Studenovský, M. Pechar, K. Ulbrich, O. Hovorka, D. Větvíčka, B. Říhová, *J. Drug Targeting* **2009**, *17*, 763.
- [5] Z.-R. Lu, S.-Q. Gao, P. Kopečková, J. Kopeček, *Bioconjugate Chem.* **2000**, *11*, 3.
- [6] J. Hongrapipat, P. Kopečková, J. Liu, S. Prakongpan, J. Kopeček, *Mol. Pharmaceutics* **2008**, *5*, 696.
- [7] B. Říhová, P. Kopečková, J. Strohalm, P. Rossmann, V. Větvíčka, J. Kopeček, *Clin. Immunol. Immunopathol.* **1988**, *46*, 100.
- [8] M. Kovář, T. Mrkvan, J. Strohalm, T. Etrych, K. Ulbrich, M. Štastný, B. Říhová, *J. Controlled Release* **2003**, *92*, 315.
- [9] T.-W. Chu, J. Kopeček, *Biomater. Sci.* **2015**, *3*, 908.
- [10] K. S. Palla, L. S. Witus, K. J. Mackenzie, C. Netirojanakul, M. B. Francis, *J. Am. Chem. Soc.* **2015**, *137*, 1123.
- [11] F. Sun, W.-B. Zhang, A. Mahdavi, F. H. Arnold, D. A. Tirrell, *Proc. Natl. Acad. Sci. USA* **2014**, *111*, 11269.
- [12] R. J. Spears, M. A. Fascione, *Org. Biomol. Chem.* **2016**, *14*, 7622.
- [13] L. S. Witus, T. Moore, B. W. Thuronyi, A. P. Esser-Kahn, R. A. Scheck, A. T. Iavarone, M. B. Francis, *J. Am. Chem. Soc.* **2010**, *132*, 16812.
- [14] S. Ulrich, D. Boturyn, A. Marra, O. Renaudet, P. Dumy, *Chem. – Eur. J.* **2014**, *20*, 34.
- [15] B. Apostolovic, M. Danial, H.-A. Klok, *Chem. Soc. Rev.* **2010**, *39*, 3541.
- [16] S. P. E. Deacon, B. Apostolovic, R. J. Carbajo, A. Schott, K. Beck, M. J. Vicent, A. Pineda-Lucena, H. Klok, R. Duncan, *Biomacromolecules* **2011**, *12*, 19.
- [17] M. Pechar, R. Pola, R. Laga, K. Ulbrich, L. Bednářová, P. Maloň, I. Siegllová, V. Král, M. Fábry, O. Vaněk, *Biomacromolecules* **2011**, *12*, 3645.
- [18] B. Apostolovic, S. P. E. Deacon, R. Duncan, H.-A. Klok, *Macromol. Rapid Commun.* **2011**, *32*, 11.



- [19] K. Wu, J. Yang, J. Liu, J. Kopeček, *J. Controlled Release* **2012**, *157*, 126.
- [20] K. Wu, J. Liu, R. N. Johnson, J. Yang, J. Kopeček, *Angew. Chem., Int. Ed.* **2010**, *49*, 1451.
- [21] T.-W. Chu, R. Zhang, J. Yang, M. P. Chao, P. J. Shami, J. Kopeček, J. Kopeček, *Theranostics* **2015**, *5*, 834.
- [22] T.-W. Chu, K. M. Kosak, P. J. Shami, J. Kopeček, *Drug Delivery Transl. Res.* **2014**, *4*, 389.
- [23] T.-W. Chu, J. Yang, R. Zhang, M. Sima, J. Kopeček, *ACS Nano* **2014**, *8*, 719.
- [24] R. A. Willemsen, M. Pechar, R. C. Carlisle, E. Schooten, R. Pola, A. J. Thompson, L. W. Seymour, K. Ulbrich, *Pharm. Res.* **2010**, *27*, 2274.
- [25] R. Pola, R. Laga, K. Ulbrich, I. Siegllová, V. Král, M. Fábry, M. Kabešová, M. Ková, M. Pechar, *Biomacromolecules* **2013**, *14*, 881.
- [26] M. Pechar, R. Pola, R. Laga, A. Braunová, S. K. Filippov, A. Bogomolova, L. Bednárová, O. Vaněk, K. Ulbrich, *Biomacromolecules* **2014**, *15*, 2590.
- [27] H. Nakamura, E. Koziolová, T. Etrych, P. Chytil, J. Fang, K. Ulbrich, H. Maeda, *Eur. J. Pharm. Biopharm.* **2014**, *90*, 90.
- [28] K. Ulbrich, V. Šubr, J. Strohalm, D. Plocová, M. Jelínková, B. Říhová, *J. Controlled Release* **2000**, *64*, 63.
- [29] R. Pola, O. Janoušková, T. Etrych, *Physiol. Res.* **2016**, *65*, 225.
- [30] S. Perrier, P. Takolpuckdee, J. Westwood, D. M. Lewis, *Macromolecules* **2004**, *37*, 2709.
- [31] T. Etrych, V. Šubr, J. Strohalm, M. Šírová, B. Říhová, K. Ulbrich, *J. Controlled Release* **2012**, *164*, 346.
- [32] H. Nakamura, E. Koziolová, P. Chytil, K. Tsukigawa, J. Fang, M. Haratake, K. Ulbrich, T. Etrych, H. Maeda, *Mol. Pharmaceutics* **2016**, *13*, 4106.
- [33] R. Laga, O. Janoušková, K. Ulbrich, R. Pola, J. Blažková, S. K. Filippov, T. Etrych, M. Pechar, *Biomacromolecules* **2015**, *16*, 2493.
- [34] M. Kovář, J. Tomala, H. Chmelová, L. Kovář, T. Mrkvan, R. Josková, Z. Zákostelská, T. Etrych, J. Strohalm, K. Ulbrich, M. Šírová, B. Říhová, *Cancer Res.* **2008**, *68*, 9875.